Laser Annealing of Sb2Te3 2D Layers towards Nonlinear Optical Applications

Delphine Coiras, Richard-Nicolas Verrone, Andrea Campos, Martiane Cabié, Laurent Gallais, Marco Minissale, Julien Lumeau, Jean-Yves Natoli, Konstantinos Iliopoulos

optics

MDPI

Article

Laser Annealing of Sb_2Te_3 2D Layers towards Nonlinear Optical Applications

Delphine Coiras [1], Richard-Nicolas Verrone [1], Andrea Campos [2], Martiane Cabié [2], Laurent Gallais [1], Marco Minissale [3], Julien Lumeau [1], Jean-Yves Natoli [1] and Konstantinos Iliopoulos [1,*]

[1] Aix Marseille Univ, CNRS, Centrale Marseille, Institut Fresnel, Marseille, France; delphine.coiras@outlook.fr (D.C.); richard-nicolas.verrone@fresnel.fr (R.-N.V.); laurent.gallais@fresnel.fr (L.G.); julien.lumeau@fresnel.fr (J.L.); jean-yves.natoli@fresnel.fr (J.-Y.N.)
[2] Aix Marseille Univ, CNRS, Centrale Marseille, FSCM (FR1739), CP2M, 13397 Marseille, France; andrea.campos@univ-amu.fr (A.C.); martiane.cabie@univ-amu.fr (M.C.)
[3] Aix Marseille Univ, CNRS, PIIM, Marseille, France; marco.minissale@univ-amu.fr
* Correspondence: konstantinos.iliopoulos@fresnel.fr

Abstract: In this work, we performed laser annealing of thin Sb_2Te_3 films to optimize crystallization time and their nonlinear optical properties. The annealed layers were studied by electron microscopy and UV–Vis spectrophotometry. Their nonlinear optical response was investigated by nonlinear transmission and Z-scan measurements. These studies were performed by a femtosecond laser system providing 400 fs laser pulses at 1030 nm. The results were compared with previous findings based on studies of oven-annealed thin films.

Keywords: chalcogenides; nonlinear optical properties; Z-scan; ultrafast saturable absorption

Citation: Coiras, D.; Verrone, R.-N.; Campos, A.; Cabié, M.; Gallais, L.; Minissale, M.; Lumeau, J.; Natoli, J.-Y.; Iliopoulos, K. Laser Annealing of Sb_2Te_3 2D Layers towards Nonlinear Optical Applications. *Optics* **2022**, *3*, 234–242. https://doi.org/10.3390/opt3030023

Academic Editor: Thomas Seeger

Received: 15 June 2022
Accepted: 12 July 2022
Published: 15 July 2022

1. Introduction

Currently, 2D materials are among the best candidates for a variety of applications including nonlinear optics and photonics [1–4]. Many interesting studies are performed every year to shed light on different aspects of these unique systems such as their structure and nonlinear optical properties as well as electron/photon interactions in their volume/surface. Our group had previously demonstrated that Sb_2Te_3 thin films can have unprecedented nonlinearities when irradiated with laser pulses. Our demonstrations were conducted in the nanosecond and femtosecond regimes in the visible and IR parts of the spectrum [5–7]. The optical nonlinearities of the Sb_2Te_3 material were employed to perform super-resolution and mode-locking of laser systems [8,9].

A significant difficulty arises during the optimization of these layers. To enhance their nonlinearities, a well-defined crystalline structure must be achieved, which requires a thorough adjustment of several parameters: the film thickness, annealing temperature/duration, obtained crystal size and crystalline structure. If one or more of these parameters are not well adjusted, the optical nonlinearities decrease significantly. Our group previously prepared Sb_2Te_3 layers by oven and laser annealing and demonstrated by means of the Z-scan technique that the nonlinearities were the highest ever reported for Sb_2Te_3 [6].

In our previous work [6] we demonstrated that a laser-annealing duration of about 45 min was necessary to achieve efficient crystallization. This was much shorter than the 24 h annealing that was employed for the oven annealing in the same work. However, even shorter annealing durations (less than 5 min) can offer more application advantages. For this reason, we focused on a systematic study of the evolution of the linear optical properties for different laser powers to show how the optical response of a material can provide a useful tool for probing a change in surface morphology. Moreover, during the current work we adjusted the laser annealing conditions to achieve much faster crystallization

while maintaining significant optical nonlinearities. First, the thin film deposition and annealing conditions are presented followed by Scanning Electron Microscopy (SEM) and Transmission Electron Microscopy (TEM) studies to confirm the presence of crystals in the thin layers. Then, to reveal the nonlinear optical efficiency of the thin layers, nonlinear transmission studies were performed in several positions inside the laser-annealed zones to provide the nonlinear efficiency as a function of the position of the probing laser beam inside the crystallized zone. These studies additionally provided confirmation of the homogeneity of the nonlinear optical responses in the central part of the crystallized zones. Finally, Z-scan studies were conducted to determine the nonlinear absorption coefficients.

2. Materials and Methods

2.1. Thin Film Deposition

The electron beam deposition technique (EBD) by a Buhler SYRUSpro 710 machine has been employed to deposit Sb_2Te_3 thin films on 1 mm thick B270 substrates. A quartz microbalance was used to measure the Sb_2Te_3 thickness with a precision of $\pm$0.2 nm. A thickness of 10 nm was chosen because we had previously demonstrated that the maximum nonlinearity for the Sb_2Te_3 material by our deposition method was between 8 and 11 nm [7]. The layers were capped by a 2 nm thick SiO_2 layer. All the samples in this work (TF1, TF2 and TF3) were deposited under the same experimental conditions so that they would be identical before the laser annealing, which is described in the next section.

2.2. Laser Annealing

To induce significant nonlinearities, the deposited samples had to be annealed. As previously mentioned, laser annealing was chosen and was carried out by a continuous wave high-power laser (AMTRON) based on a fiber-coupled GaAs diode emitting at 805 nm (JENOPTIK Laser GmbH). The setup used for the annealing is briefly presented here; detailed information can be found elsewhere [10]. A pump–probe configuration was used to allow crystallization by in situ detection of the reflectance and temperature of the samples. The power of the laser beam was adjusted by using filters and a combination of a half wave-plate and a polarizer. The beam used for the annealing exhibited a super gaussian spatial profile and its diameter was measured to be 3.4 mm at the sample position. The annealing occurred mainly due to laser heating. During the annealing, the temperature on the irradiated zone was detected by a thermal camera (FLIR A655) using a 0.7 emissivity. The camera operated in the 7.4–14 μm wavelength range.

Probing the crystallization evolution was done during the annealing by means of a supercontinuum laser (Leukos Samba). The probe beam diameter was measured to be 1.5 mm. A smaller beam with respect to the pump beam was chosen to allow detection of the reflectance in the central part of the annealed region. The laser irradiated the sample, and the reflected part of the beam was detected by an integrating sphere and a spectrometer (Avantes Evo XL). Based on the spectrometric data, in situ detection of the reflectance of the annealed samples was feasible. A 70 mW supercontinuum laser was chosen to avoid any further interaction with the Sb_2Te_3 material. The stability of the Sb_2Te_3 material upon the supercontinuum irradiation has been confirmed prior to the measurements by irradiating the samples only using the supercontinuum light source while detecting their reflectance. The reflectance, which is well-known to be strongly related with the crystalline structure of the Sb_2Te_3 material, was unchanged during several hours of irradiation with the probe beam, proving that no modification of the samples occurred during the probing.

2.3. Electron Microscopy

The crystalline structure of the materials was studied by means of SEM (Zeiss Gemini500) and TEM (FEI Tecnaï G2).

The SEM images were acquired using a four quadrant backscattered electron (BSE) detector, which can be used to image crystallographic contrast: the BSE intensity varies

according to the crystal orientation. The electron acceleration voltage adequate to observe the Sb_2Te_3 layer was 10 kV.

The TEM analysis was performed at 200 kV. Dark field conventional images, diffraction patterns as well as high resolution images were acquired to compare the degree of crystallinity in each sample. For TEM analysis, after scraping the sample surface with a metal tip, the layer debris was collected on the carbon membrane of a copper grid by dabbing the grid on the etched area. For the sample TF3 only, cross-sectional images of the layer were observed on a lamella prepared by a focused ion beam (FIB) (FEI, dual beam Helios 600 Nanolab).

2.4. Nonlinear Optical Studies

For the nonlinear optical studies, a femtosecond laser system was employed (Amplitude Systems, Yuja), delivering 400 fs duration pulses at 1030 nm. The repetition rate of the laser was adjusted at 100 Hz to avoid thermal effects that can arise while irradiating with higher repetition rates [11]. Two different studies were conducted to determine the nonlinear optical response of the samples. Firstly, nonlinear transmission studies were carried out. In this case, the sample was positioned at the focal plane of a focusing lens and it has been irradiated with different laser intensities to find the transmittance modification due to the femtosecond irradiation. Then, Z-scan measurements were performed to determine the nonlinear optical parameters. The Z-scan technique is described in detail elsewhere [12,13] so a brief description will be done here. The laser beam was focused by a 10 cm focal length lens on the sample, which was moved around the focal plane by means of a motorized translation stage. The beam waist at the focal plane was measured to be 20 μm. During the measurements, the transmission of the material was simultaneously measured by two different experimental arms, the so-called "closed aperture" and "open aperture" Z-scans, which offered information concerning nonlinear refraction and absorption, respectively.

Our group had previously demonstrated that Sb_2Te_3 films thicker than 6 nm exhibit significant nonlinear absorption, while nonlinear refraction is negligible [7]. For this reason, in the case of the 10 nm thick Sb_2Te_3 films studied in this work, the open aperture recordings were of main interest. The nonlinear absorption coefficient β was determined by fitting the open aperture Z-scan curves by means of Equation (1):

$$T = \frac{1}{\sqrt{\pi}\left(\frac{\beta I_0 L_{eff}}{1+z^2/z_0^2}\right)} \int_{-\infty}^{\infty} \ln\left[1 + \frac{\beta I_0 L_{eff}}{1+z^2/z_0^2}\exp\left(-t^2\right)\right] dt \quad (1)$$

where I_0 is the on-axis irradiance at the focus; Leff is defined as Leff = $(1 - \exp(-\alpha_0 L))/\alpha_0$; and α_0 is the linear absorption coefficient of the sample at 1030 nm. The $\mathrm{Im}\chi^{(3)}$ can be then determined by means of the following Equation:

$$\mathrm{Im}\,\chi^{(3)}(\mathrm{esu}) = \frac{10^{-7} c^2 n_0^2}{96\,\pi^2 \omega}\beta\left(\mathrm{cm\ W^{-1}}\right) \quad (2)$$

where c is the speed of light in cm s^{-1}, n_0 is the linear refractive index and ω is the fundamental frequency in cycles per sec.

3. Results

The Sb_2Te_3 thin films were crystallized using the experimental setup described in Section 2.2. The first study had a dual purpose: to estimate the power threshold required to trigger the crystallization and to determine if higher powers result in modifications to the reflectance of the layers and consequently their crystallization state. For this reason, the same zone on the thin film (thin film 1: TF1) was irradiated with increasing laser power. More specifically, the power for the irradiation ranged from 0.5 to 2.3 W with a step of 0.2–0.3 W, while a 10 min laser irradiation was performed for each power. This range of powers was employed because it was found to result in efficient annealing and

allowed to avoid modification and damage to the layers, which has been found to arise for laser powers higher than 3.5 W. The reflectance as a function of the wavelength was recorded throughout the annealing procedure in the 500–1100 nm range, as described in Section 2.2. In Figure 1a, representative curves of the reflectance at 900 nm are represented as a function of the irradiation time for different annealing powers. This wavelength was arbitrarily chosen; similar behaviors were obtained for the other wavelengths in this range. No modification of the crystalline state was found during irradiation carried out by using laser powers lower than 1 W. However, when the sample was irradiated by 1.1 W, a gradual increase in reflectance was observed, as would be expected for a Sb_2Te_3 thin film passing from an amorphous to a crystalline state [14]. A reflectance maximum was obtained about 7 min after starting the annealing. No further modification of the layer reflectance was observed after reaching this maximum; that is, for an annealing duration longer than 7 min. Additionally, when the same zone was irradiated with higher laser power (1.3–2.3 W), the reflectance remained the same, indicating that an optimal annealing had already been obtained using 1.1 W. It should be noted that for all the recorded curves, an initial decrease in reflectance was observed during the first seconds of laser annealing. This decrease, which occurred even at low power, was not attributed to a change of the crystalline state of the materials but to a modification in the reflectance as a function of the temperature of the Sb_2Te_3 sample, which our group had previously observed [6].

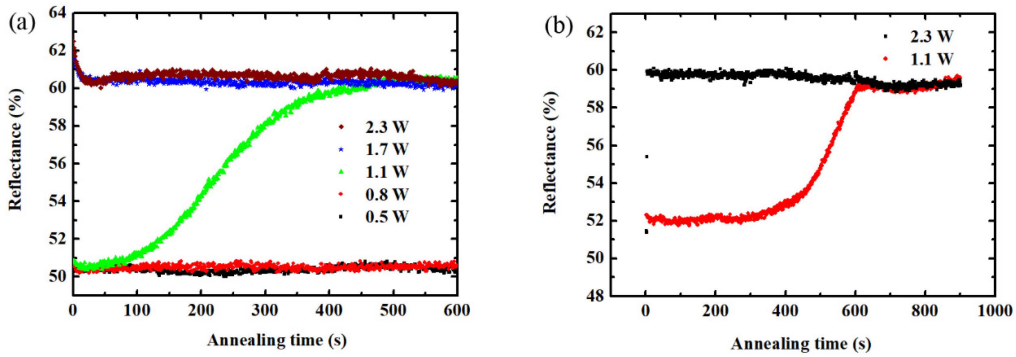

Figure 1. Reflectance as a function of the annealing time obtained in the case of the (**a**) TF1, (**b**) TF2 and TF3 layers.

It has to be noted that the optical response of a material (e.g., its reflectivity) is directly related to the motion of electrons in the conduction band and to the damping mechanisms (i.e., electron–electron and electron–phonon scattering) that transferred energy from the laser to the sample. In our case, we observed a temperature increase of around 200 °C in the first seconds of the laser annealing. Since both the motion of the electrons and the damping mechanisms depend on the temperature, the optical properties were modified due to variation in the sample temperature in this first phase, which explained the decrease of the reflectance during the first seconds of irradiation. Another annealing study was carried out to discover if faster crystallization than that obtained by 1.1 W laser power can be achieved by directly irradiating a Sb_2Te_3 sample with higher laser powers. A comparative study in this case was performed on two thin films using single laser power annealing for each film. In the first case, a 1.1 W laser power was chosen (thin film 2: TF2), while 2.3 W laser power was employed in the second (thin film 3: TF3). The results of this comparative study can be seen in Figure 1b. Three different facts have to be highlighted. Firstly, in the case of the low power irradiation, a 10 min annealing was necessary. This duration is higher than that obtained for the previous irradiation (7 minutes, see Figure 1a). This difference can be attributed to the fact that the sequence of crystallizations performed under low power, in the case of the study shown in Figure 1a, did not result in a detectable crystallization change but rather accelerated the annealing that took place under 1.1 W. Moreover, in the direct annealing case using a 2.3 W laser (Figure 1b), a very fast crystallization was

obtained. Indeed, a 5 s annealing was sufficient to obtain a reflectance maximum, while no significant reflectance changes were observed for longer annealing durations. Finally, the initial decrease of the reflectance due to the temperature increase was not visible due to the fast increase in reflectance linked to the rapid crystallization, which masked the former, less-significant effect. As mentioned in Section 2.2, the temperature of the sample was monitored by a thermal camera throughout the annealing. The maximum temperatures attained in the case of the TF2 and TF3 samples were 80 and 217 °C respectively.

After the annealing, Vis-NIR spectrophotometric studies from 400 to 1200 nm were performed by a PerkinElmer Lambda 1050. Representative curves of the reflectance and transmittance of the annealed and amorphous zones of the TF3 sample can be seen in Figure 2, and very similar spectra were recorded for the other samples. More specifically, the red curves correspond to the transmittance and the black to the reflectance. In the same figure, the dashed and continuous lines correspond to the amorphous and crystalline zones, respectively. The values obtained at 1030 nm were taken into account during the analysis of the nonlinear optical data. It should be noted that the reflectance value of the sample at 900 nm was different from that presented in Figure 1 because of the different angles of incidence employed during the laser annealing and spectrophotometric studies.

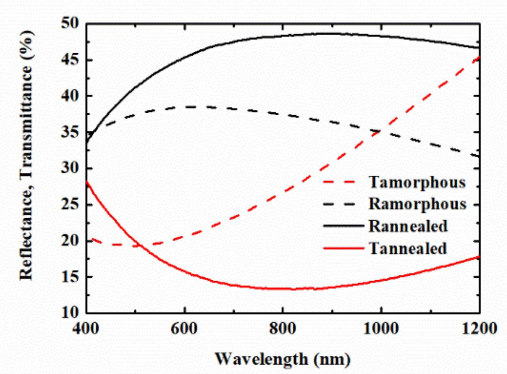

Figure 2. Reflectance and transmittance spectra for the amorphous and annealed zones of the thin films.

Scanning electron microscopy studies were additionally performed inside and outside the annealed zones. Many images were recorded for each sample at different positions in the crystallized zones. Representative results, obtained in the case of the TF1 film can be seen in Figure 3. One can note a high density of crystals in the central part of the annealed zone (Figure 3a).

These grains of a size smaller than 30 nm were also observed on dark field TEM images (Figure 4a). In addition, the diffraction pattern showed rings with distances coherent with the rhombohedral crystalline structure of the Sb_2Te_3 phase (Figure 4b).

An HRTEM image observed on a cross-section of sample TF3 prepared by FIB revealed the presence of lattice fringes 0.321 nm distant (Figure 3f), corresponding to (015) planes. This image also confirmed that the layer was well crystallized. The measured layer thickness is equal to 14 $\pm$ 2 nm. The difference between the thicknesses stated here for the annealed samples and those given in Section 2.1 for the amorphous layers can be attributed to the crystallization, which resulted in slightly rough surfaces due to the transfer of matter during the annealing.

The shape of the crystals was found to be different a few millimeters away from the center, see for example an image obtained 2.3 mm away from the center in Figure 3b. This shape difference resulted in a significant loss in nonlinear absorption, which is presented in the next paragraphs. Near the border of the crystallized zone (Figure 3c,d), the crystal density was significantly reduced. Outside the annealed zone, no crystals were observed (Figure 3e). The optical nonlinearities obtained near the border and outside the annealed zone were found to be negligible.

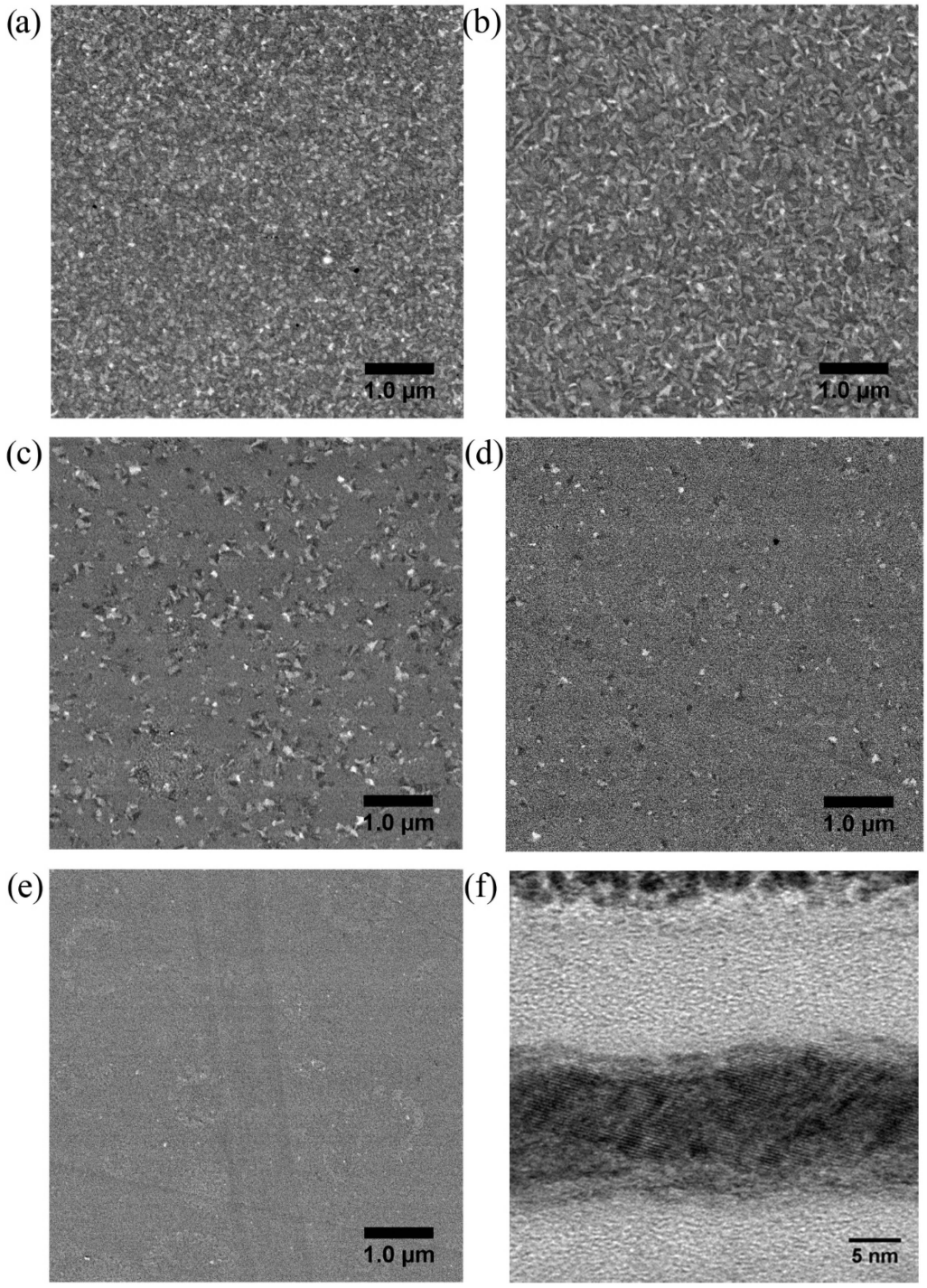

Figure 3. (**a**) Scanning electron microscopy images of the TF1 film recorded at (**a**) the center of the crystallized zone, (**b**) 2.3 mm from the center, (**c**) 5.1 mm from the center, (**d**) 5.2 mm from the center, (**e**) outside the annealed zone. The radius of the crystallized zone is 5.5 mm. (**f**) HRTEM image of a cross-section of sample TF3 prepared by FIB.

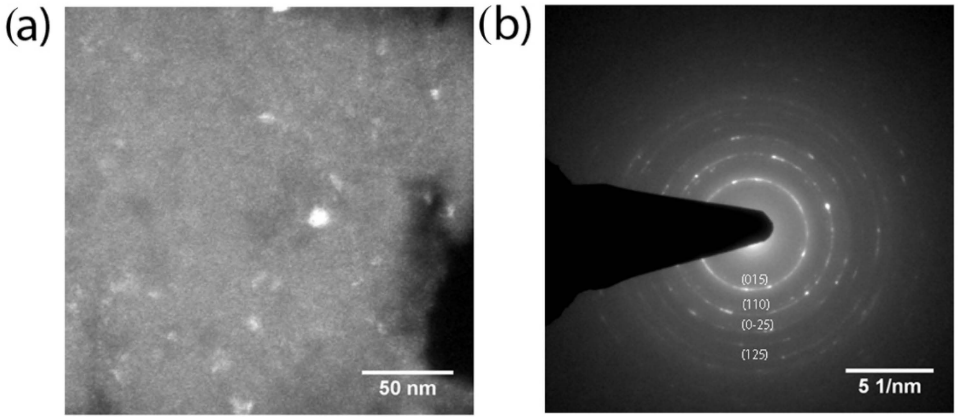

Figure 4. (**a**) A dark field TEM plan view image. Crystalline grains in Bragg position appear bright. (**b**) Diffraction pattern of the area in the left image.

After the thin film layers were prepared and characterized, nonlinear optical studies were performed. The first study determined the nonlinear transmission inside the laser-crystallized zones of the samples, which had been scanned by a 40 µm diameter laser beam. For each position of the laser beam in the crystallized area, the following procedure was followed: Firstly, a weak laser intensity (0.04 GW/cm^2) was used to determine the linear transmittance of the sample. An increase in transmission, while scanning the sample from the center to the edge of the crystallized area, was observed and was attributed to the Gaussian spatial profile of the laser beam used for the annealing. This variation in transmission was taken into account during the next step of the analysis.

Using a higher intensity (3 GW/cm^2), the saturable absorption character of the samples was activated, resulting in an increase in the transmission of the Sb_2Te_3 layers. The transmission of the sample at the high intensity regime divided by the transmission obtained at the low intensity regime provided the normalized transmittance, which is presented in Figure 5a,b for the samples TF1 and TF3, respectively. As can be seen in these figures, the optical nonlinearities were significant in a zone having a diameter of about 1 cm, which matches the size of the crystallized zone. Outside this zone, the optical nonlinearities were found to be negligible, so the normalized transmittance was equal to unity. It can be seen that the maximum transmittances were similar for the samples TF1 and TF3: about 1.08. The average nonlinear absorption coefficient (β) of the central part of the annealed zones was calculated based on the measured nonlinear transmissions and using the expressions shown in Section 2.4. It was found to be -1.7×10^{-6} and -1.6×10^{-6} m/W for thin films TF1 and TF3, respectively. In the case of the TF2 sample, the lower power (1.1 instead of 2.3 W) resulted in a smaller crystallized zone (radius less than 0.2 cm) which would render a study imprecise. By comparing these results with the SEM images in Figure 4, it was noted that the shape of the crystals and their density had a high impact on the optical nonlinearities. Indeed, near the center of the annealed zone, a high saturable absorption was obtained, but it gradually decreased as the laser beam moved towards the border of this zone.

To provide a more precise determination of the nonlinear absorption coefficients of the annealed thin films, Z-scan studies were performed in the center of the crystallized areas. A very good alignment of the experimental setup was necessary to make sure that the sample was always at normal incidence. In this way, the laser beam irradiated the same area of the sample, while moving along the Z-axis of the setup. Two representative open aperture Z-scan curves are shown in Figure 6a,b for thin films TF1 and TF3, employing 4.3 and 3.0 GW/cm^2, respectively. In both cases, a transmission peak was acquired, revealing the saturable absorption behavior of the investigated thin films. The nonlinear absorption coefficients were determined by fitting the results with the models presented in Section 2.4 and found to be -2.3×10^{-6} m/W for both TF1 and TF3.

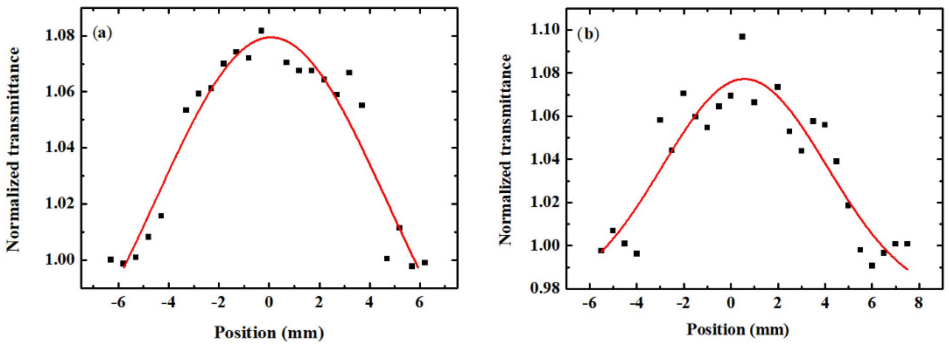

Figure 5. Normalized transmittance as a function of the position of the probe beam inside the laser annealed zone in the case of the (**a**) TF1 and (**b**) TF3 samples.

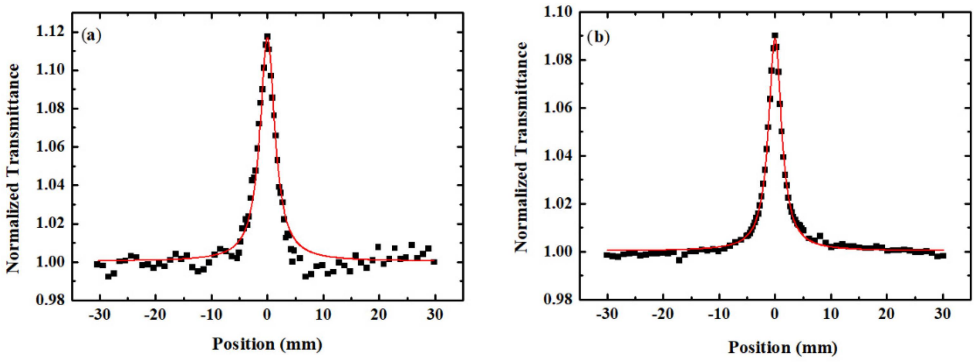

Figure 6. Representative open aperture Z-scan curves recorded for the (**a**) TF1 and (**b**) TF3 samples.

These values were in good accordance with those determined by the nonlinear transmission study. The difference between the values obtained from the two studies can be attributed to the fact that during a Z-scan study the same spot on the sample was irradiated throughout the scan, while in the case of the nonlinear transmission analysis, the β value was determined by averaging over many different measurements obtained at different sample positions in the central part of the crystallized zone. The inhomogeneities of the crystalline structure due to the Gaussian beam profile employed for the annealing gave rise to this difference. The values obtained were also in very good agreement with previous results reported by our group. In reference [7], we performed a thickness-dependent nonlinear optical study of Sb_2Te_3 thin films. The nonlinear absorption coefficient for thin films of the same thickness (10 nm) was -1.5×10^{-6} m/W. This value was slightly lower than those obtained in this work, which can be attributed to the different annealing methods employed. In our previous work, oven annealing was employed, while here it was a laser annealing. However, the setup that was employed (Z-scan) and the experimental conditions were identical between the two works, so a direct comparison of the results is feasible. A detailed comparison of the optical nonlinearities of the Sb_2Te_3 thin films prepared by our group and the results of other scientific groups on highly efficient photonic materials had been previously presented (see reference [6] and Table 1 therein).

4. Conclusions

Thin Sb_2Te_3 films were laser-annealed to induce high optical nonlinearities. The laser power was adjusted to accelerate and optimize their crystallization. In the case of a 2.3 W annealing, a very fast crystallization was obtained (5 s). The annealed thin films were studied by nonlinear transmission and Z-scan to determine their nonlinear optical parameters.

Author Contributions: Conceptualization, K.I., M.M., J.-Y.N. and J.L.; formal analysis, A.C., M.C., L.G., D.C. and R.-N.V.; investigation, A.C., M.C., D.C. and R.-N.V.; data curation, K.I. and M.M.;

writing—original draft preparation, K.I. and M.M.; writing—review and editing, K.I., M.M., J.-Y.N., J.L., L.G., M.C. and A.C; supervision, K.I., M.M., J.-Y.N. and J.L.; All authors have read and agreed to the published version of the manuscript.

Funding: This research was funded by the French National Research Agency, grant number (ANR-19-CE09-0002-01), from the Ministry for Armed Forces (DGA), and Aix-Marseille University.

Institutional Review Board Statement: Not applicable.

Informed Consent Statement: Not applicable.

Conflicts of Interest: The authors declare no conflict of interest.

References

1. Liu, W.; Liu, M.; Liu, X.; Wang, X.; Deng, H.; Lei, M.; Wei, Z.; Wei, Z. Recent Advances of 2D Materials in Nonlinear Photonics and Fiber Lasers. *Adv. Opt. Mater.* **2020**, *8*, 1901631. [CrossRef]
2. Guo, B.; Xiao, Q.; Wang, S.; Zhang, H. 2D Layered Materials: Synthesis, Nonlinear Optical Properties, and Device Applications. *Laser Photonics Rev.* **2019**, *13*, 1800327. [CrossRef]
3. Wang, G.; Baker-Murray, A.A.; Blau, W.J. Saturable Absorption in 2D Nanomaterials and Related Photonic Devices. *Laser Photonics Rev.* **2019**, *13*, 1800282. [CrossRef]
4. Autere, A.; Jussila, H.; Dai, Y.; Wang, Y.; Lipsanen, H.; Sun, Z. Nonlinear Optics with 2D Layered Materials. *Adv. Mater.* **2018**, *30*, 1705963. [CrossRef] [PubMed]
5. Moisset, C.; Bourgade, A.; Lumeau, J.; Lemarchand, F.; Perrin-Pellegrino, C.; Akhouayri, H.; Natoli, J.-Y.; Iliopoulos, K. Saturable Absorption Optimization of Silica Protected Thin Sb_2Te_3 Layers towards Super-Resolution Applications. *Opt. Mater.* **2018**, *86*, 7–11. [CrossRef]
6. Moisset, C.; Verrone, R.-N.; Bourgade, A.; Zeweldi, G.T.; Minissale, M.; Gallais, L.; Perrin-Pellegrino, C.; Akhouayri, H.; Lumeau, J.; Natoli, J.-Y.; et al. Giant Ultrafast Optical Nonlinearities of Annealed Sb_2Te_3 Layers. *Nanoscale Adv.* **2020**, *2*, 1427–1430. [CrossRef]
7. Verrone, R.-N.; Moisset, C.; Lemarchand, F.; Campos, A.; Cabié, M.; Perrin-Pellegrino, C.; Lumeau, J.; Natoli, J.-Y.; Iliopoulos, K. Thickness-Dependent Optical Nonlinearities of Nanometer-Thick Sb_2Te_3 Thin Films: Implications for Mode-Locking and Super-Resolved Direct Laser Writing. *ACS Appl. Nano Mater.* **2020**, *3*, 7963–7972. [CrossRef]
8. Wang, Z.; Li, C.; Ye, J.; Wang, Z.; Liu, Y.-G. Generation of harmonic mode-locking of bound solitons in the ultrafast fiber laser with Sb_2Te_3 saturable absorber on microfiber. *Laser Phys. Lett.* **2019**, *16*, 025103. [CrossRef]
9. Sotor, J.; Sobon, G.; Macherzynski, W.; Paletko, P.; Grodecki, K.; Abramski, K. Mode-locking in Er-doped fiber laser based on mechanically exfoliated Sb_2Te_3 saturable absorber. *Opt. Mater. Express* **2013**, *4*, 1–6. [CrossRef]
10. Minissale, M.; Pardanaud, C.; Bisson, R.; Gallais, L. The Temperature Dependence of Optical Properties of Tungsten in the Visible and Near-Infrared Domains: An Experimental and Theoretical Study. *J. Phys. D Appl. Phys.* **2017**, *50*, 455601. [CrossRef]
11. Karampitsos, N.; Kyrginas, D.; Couris, S. On the Measurement of the Nonlinear Optical Response of Graphene Dispersions Using Fs Lasers. *Opt. Lett.* **2020**, *45*, 1814. [CrossRef] [PubMed]
12. Sheik-Bahae, M.; Said, A.A.; Wei, T.-H.; Hagan, D.J.; Van Stryland, E.W. Sensitive Measurement of Optical Nonlinearities Using a Single Beam. *IEEE J. Quantum Electron.* **1990**, *26*, 760–769. [CrossRef]
13. Iliopoulos, K.; El-Ghayoury, A.; El Ouazzani, H.; Pranaitis, M.; Belhadj, E.; Ripaud, E.; Mazari, M.; Sallé, M.; Gindre, D.; Sahraoui, B. Nonlinear Absorption Reversing between an Electroactive Ligand and Its Metal Complexes. *Opt. Express* **2012**, *20*, 25311–25316. [CrossRef] [PubMed]
14. Fujimori, S.; Yagi, S.; Yamazaki, H.; Funakoshi, N. Crystallization Process of Sb-Te Alloy Films for Optical Storage. *J. Appl. Phys.* **1988**, *64*, 1000. [CrossRef]